ChemComm

Accepted Manuscript

This article can be cited before page numbers have been issued, to do this please use: N. Leconte, J. Moutet, K. Herasymchuk, R. Clarke, C. Philouze, D. Luneau, T. Storr and F. Thomas, *Chem. Commun.*, 2017, DOI: 10.1039/C7CC00516D.

ROYAL SOCIETY OF CHEMISTRY

rsc.li/chemcomm

View Article Online
DOI: 10.1039/C7CC00516D

Journal Name

COMMUNICATION

Mn(IV) and Mn(V)-radical Species Supported by the Redox Non-innocent bis(2-amino-3,5-di-*tert*-butylphenyl)amine Pincer Ligand

Received 00th January 20xx,
Accepted 00th January 20xx

DOI: 10.1039/x0xx00000x

www.rsc.org/

N. Leconte[a]*, J. Moutet[a], K. Herasymchuk,[b] R. M. Clarke,[b] C. Philouze[a], D. Luneau,[c] T. Storr,[b] F. Thomas[a]*

The electron-rich pincer ligand 1 has been synthesized and chelated to manganese. The octahedral Mn(IV) bis(diiminosemiquinonate) and Mn(V) (diiminobenzoquinone) (diiminosemiquinonate) radicals were structurally characterized.

The coordination chemistry of redox non-innocent ligands based on aniline and phenylenediamine moieties is of current interest.[1-3] The diaminobenzene entity is among the most electron-rich organic compounds[4] and subsequently the precursor of stable *N*-centered radicals, the most famous being the Wurzter's salt (*p*-phenylene bis(dimethylamine) radical) reported over one century ago.[5] While there is no ambiguity regarding the charge distribution in the free radical, its use as a ligand dramatically complicates the assignment of the electronic structure. The close similarity between the metal-centered and ligand-centered redox active orbitals can indeed allow for complete charge redistribution. While the coordination chemistry of pincer ligands based on the bis(3,5-di-*tert*-butyl-2-hydroxyphenyl)amine platform has been well documented since the original work of Girgis and Balch,[6] metal complexes involving the bis(2-aminophenyl)amine platform have been reported only very recently.[7,8] For instance, Hu *et al.* prepared nickel(II) complexes from the ligand N_2N depicted in Fig. 1, which were used as catalysts for C-C bond formation. While single or double oxidation of the complex would produce formally a Ni(III) or Ni(IV) species, the authors suspected, but did not definitively demonstrate, that the ligand might be oxidized instead of the metal. [7] Heyduk *et al.* reported catalysts for nitrene transfer using a related pincer type ligand (NNN^{Cat}, Fig. 1) coordinated to tantalum(V) and zirconium(IV). They unambiguously established that the ligand alone supports the electron transfers during catalysis, by shuttling between the diamidobenzene and diiminobenzoquinone oxidation states. [8]

We herein describe a new pincer ligand, bis(2-amino-3,5-di-*tert*-butylphenyl)amine **1**, and its manganese complexes $\mathbf{2}^{0/2+}$. The four *tert*-butyl groups make **1** considerably electron rich, stabilizing high oxidation states of the complexes. The structures of **2** and $\mathbf{2}^{2+}$ are consistent with Mn(IV) bis(radical) and Mn(V) radical species, respectively.

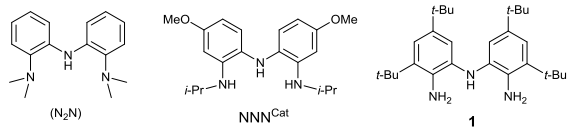

Figure 1 Structures of pincer ligands involving *o*-phenylenediamine donors

The synthetic route to **1** involves a Pd-catalyzed *N*-arylation between 3,5-di-*tert*-butyl-2-nitroaniline **3** and the previously described *o*-nitrobromobenzene derivative **4** (Scheme 1).[2i] The reaction is performed in the presence of a catalytic amount of Pd_2dba_3/*rac*-BINAP and Cs_2CO_3 as the base. In these conditions the nitro intermediate **5** is obtained in a 99% yield and a subsequent catalytic hydrogenation over Pd/C affords the desired ligand **1** in an 88% yield.

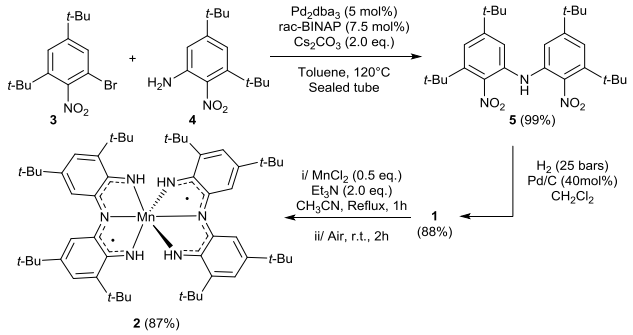

Scheme 1 Synthesis of the ligand **1** and the manganese complex **2**.

The redox non-innocence of the ligand **1** was established by cyclic voltammetry (CV, Fig. S4) since it displays two oxidation waves at

[a] *Département de Chimie Moléculaire - Chimie Inorganique Redox (CIRE) - UMR CNRS 5250, UniversitéJoseph Fourier, B. P. 53, 38041 Grenoble cedex 9, France. Email : nicolas.leconte@univ-grenoble-alpes.fr, fabrice.thomas@univ-grenoble-alpes.fr.*
[b] *Department of Chemistry, Simon Fraser University, Burnaby, British Columbia V5A 1S6, Canada.*
[c] *Laboratoire des Multimatériaux et Interfaces (UMR CNRS 5615), Université Claude Bernard Lyon 1, 69622 Villeurbanne cedex, France.*

† Electronic Supplementary Information (ESI) available: CCDC-1406874 and 1406875, experimental details, EPR and UV-Vis-NIR spectra, cyclic voltammetry curves. See DOI: 10.1039/c000000x/.

$E_{1/2}^1$ = -0.16 V (ΔEp = 0.40 V) and $E_{1/2}^2$ = +0.63 V (ΔEp = 0.15 V).[9] The reaction of **1** with 0.5 molar equivalent of $MnCl_2$ in the presence of 2 equivalents of Et_3N affords the neutral complex **2**, which was isolated as a dark powder in an 87% yield. The ESI-MS spectrum of **2** displays a prominent molecular ion peak at m/z = 896.5, whose mass and isotope distribution pattern are consistent with the presence of two deprotonated ligands coordinated to a single metal ion. IR spectroscopy shows a single N-H stretching band at 3420 cm^{-1}, confirming the deprotonation of the aniline moieties. Further, complex **2** is characterized by two broad NIR absorption bands at 1200 (4370 M^{-1} cm^{-1}) and 1800 nm (2170 M^{-1} cm^{-1}), which are reminiscent of manganese-radical species (Fig. S6).[10,11]

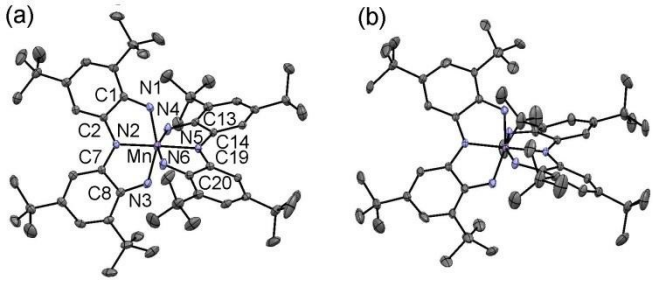

Figure 2 X-Ray crystal structures of (a) **2** and (b) $\mathbf{2}^{2+}$ (H atoms omitted for clarity)

Table 1. Selected bond distances in **2** and $\mathbf{2}^{2+}$ [a]

Bond	2	2^{2+}	Bond	2	2^{2+}
Mn-N1	1.952(2)	1.917(3)	Mn-N4	1.950(2)	1.919(2)
Mn-N2	1.922(2)	1.910(3)	Mn-N5	1.923(2)	1.911(3)
Mn-N3	1.951(2)	1.917(3)	Mn-N6	1.947(2)	1.919(2)
C1-N1	1.341(3)	1.326(4)	C13-N4	1.341(3)	1.326(4)
C8-N3	1.346(3)	1.326(4)	C20-N6	1.348(3)	1.326(4)
C2-N2	1.376(2)	1.368(3)	C14-N5	1.380(3)	1.370(3)
C7-N2	1.386(2)	1.368(3)	C19-N5	1.371(2)	1.370(3)

[a] In order to facilitate comparison the numbering of **2** is extrapolated to $\mathbf{2}^{2+}$.

Single crystals of **2** were grown under argon atmosphere by vapour diffusion of acetonitrile into a benzene solution. The structure of **2** (Fig. 2a) displays a manganese ion in a distorted octahedral geometry, coordinated to two deprotonated ligand molecules. The coordination bond distances in **2** are relatively short (Mn-N1: 1.952(2); Mn-N2: 1.922(2); Mn-N3: 1.951(2); Mn-N4: 1.950(2); Mn-N5: 1.923(2) and Mn-N6: 1.947(2) Å) and within the range of those expected for Mn(IV) complexes.[11] Furthermore, the absence of strong Jahn Teller distortion clearly rules out a Mn(III) oxidation state. The C1-N1 (1.341(3) Å), C8-N3 (1.346(3) Å), C13-N4 (1.341(3) Å) and C20-N6 (1.348(3) Å) bond distances are intermediate between those commonly observed in diamidobenzene and diiminobenzoquinone rings,[2,8,12] indicating that each ligand coordinates the Mn(IV) ion under its π-radical dianionic form. The similarity in the C1-N1, C8-N3, C13-N4 and C20-N6 bond distances discloses that the spin density is delocalized over both aromatic rings.

The X-Band EPR spectrum of **2** is independent of temperature over the 6-120 K range. It covers a relatively sharp spectral window around g ≈ 2, reflecting a (S_{tot} = ½) ground spin state for the complex (Fig. 3a). Simulation affords the spin Hamiltonian parameters $g_{\perp}$ = 2.043 and $g_{//}$ = 1.975 with $A_{\perp}$ = 5.9 and $A_{//}$ = 15.0 mT for a single Mn nucleus (I_{Mn} = 5/2), which closely match those reported by Pierpont *et al.* for the Mn(IV) bis(radical) species Mn^{IV}(Cat-N-ISQ)$_2$ ($g_{\perp}$ = 2.040 and $g_{//}$ = 1.977 with $A_{\perp}$ = 8.4 and $A_{//}$ = 15.3 mT).[10a] Thus, the observed (S_{tot} = ½) spin state arises from an antiferromagnetic interaction between each radical spin (S_{rad} = ½) and the metal spin (S_{Mn} = 3/2).[11c] Assuming that its magnitude is larger than the magnetic interaction between the two radical spins, the complex acquires a metal-based (S_{tot} = ½) ground state, resulting in the substantial hyperfine interaction with the ^{55}Mn nucleus experimentally observed. This doublet ground spin state for **2** was ascertained by DFT calculations (Fig. S8). The sextet $^6\mathbf{2}$, which consists of a high spin Mn(IV) coordinated to two ligand radicals indeed lies 21.9 kcal/mol above the broken symmetry (BS) doublet $^2\mathbf{2}$.

The CV curve of **2** exhibits one reduction wave at $E_{1/2}^1$ = -1.48 V, which is assigned to the Mn^{IV}/Mn^{III} redox couple. Three reversible oxidation waves are observed at $E_{1/2}^2$ = -0.54 V, $E_{1/2}^3$ = 0.12 V and $E_{1/2}^4$ = 0.49 V (Fig. S9). These oxidation potentials are significantly lower than those reported for manganese(IV) complexes involving the bis(3,5-di-*tert*-butyl-2-hydroxyphenyl)amine ligand.[6c] Thus, **1** is a stronger donor, with an enhanced propensity to stabilize high oxidation states of the complexes. The reversibility of the waves is also indicative of enhanced stability of the oxidized species.

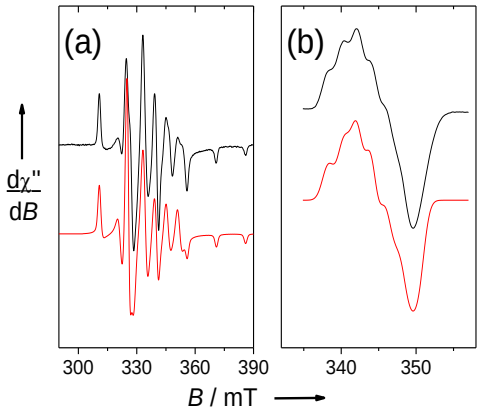

Figure 3 EPR spectra of 0.5 mM CH_2Cl_2 (+0.1 M TBAP) solutions of (a) **2** and (b) electrogenerated $\mathbf{2}^{2+}$. Microwave freq. 9.63 GHz, power 4 mW, Mod Amp. 0.4 mT, Freq. 100 KHz, *T* = 20 K (a) and 37 K (b).

The reaction of **2** with 2 eq. of $AgSbF_6$ affords the complex $\mathbf{2}^{2+}$ • 2 SbF_6^-, which is remarkably stable in CH_2Cl_2 solution (no decomposition was observed after several days). The electronic spectrum of $\mathbf{2}^{2+}$ is dominated by transitions at 400 (13 300 M^{-1} cm^{-1}), 490 (10 190 M^{-1} cm^{-1}) and 705 nm (13 830 M^{-1} cm^{-1}), together with a featureless NIR tail (Fig. S6). Complex $\mathbf{2}^{2+}$ • 2 SbF_6^- could be isolated as single crystals for structural characterization (Fig. 2b). The manganese ion retains its octahedral geometry in $\mathbf{2}^{2+}$, but the coordination sphere is globally contracted with respect to **2** (mean shortening of 0.025 Å, Table 1), indicative of a higher oxidation state of the metal. Noteworthy, all the terminal NH groups are H-bonded with SbF_6^- molecules present in the crystal cell (N-F distances at 3.18 Å). Further, the C1-N1, C8-N3, C13-N4 and C20-N6 bonds, which reflect the oxidation state of the ligand, are shorter in

2^{2+} than in **2** (by 0.015-0.02 Å), as expected for the oxidation of a single ligand molecule and delocalization of the charge over the rings.[12]

High-resolution X-Ray photoelectron spectroscopy (XPS) can provide valuable information about the formal metal oxidation state. The $Mn2p_{3/2}$ and $Mn2p_{1/2}$ binding energies (BE) for both **2** and **2^{2+}** are observed as broad multiplets 0.3 eV and 0.6 eV apart (Fig. S11-12), respectively. The broadening of the Mn2p peaks of both **2** and **2^{2+}** is due to the interaction of the Mn2p unpaired electrons (resulting from the ejection of the photoelectron) with the Mn3d electrons, producing "multiplet splitting" patterns.[13] The shift to higher BE observed upon oxidation of **2** to **2^{2+}** is attributed to an increase in oxidation state from Mn^{IV} to Mn^{V}. While very little XPS data is available for the Mn^{V} oxidation state,[14-17] recent work on $Mn^{IV/V}$ clusters[15] and Mn^{IV} complexes[17] reported a difference of <1 eV in $Mn2p_{3/2}$ BE between each consecutive oxidation state. Hence, both XRD and XPS support a Mn(V)-iminosemiquinonate formulation of **2^{2+}**.

DFT calculations on the dication **2^{2+}** are fully consistent with XRD and XPS, providing two electronic solutions with a spin density (SD) on Mn of *ca.* 2 (Fig. S13).[18] One corresponds to a high spin Mn(V) center ferromagnetically coupled to a ligand radical (quartet **^{4}[2]$^{2+}$**) while the other is a high spin Mn(V) center anti-ferromagnetically coupled to a ligand radical (doublet **^{2}[2]$^{2+}$**). Interestingly, the extent of ligand radical delocalization differs between **^{2}[2]$^{2+}$** and **^{4}[2]$^{2+}$**. In **^{2}[2]$^{2+}$** the ligand spin density (SD) is distributed in an inequivalent fashion over the two ligand moieties (-0.76 and 0.1 on each). For the quartet **^{4}[2]$^{2+}$**, the SD is equally distributed over the two ligand moieties (-0.50 on each). The **^{2}[2]$^{2+}$** and **^{4}[2]$^{2+}$** solutions are predicted to be essentially isoenergetic, the quartet solution being favoured by only 0.3 kcal/mol.

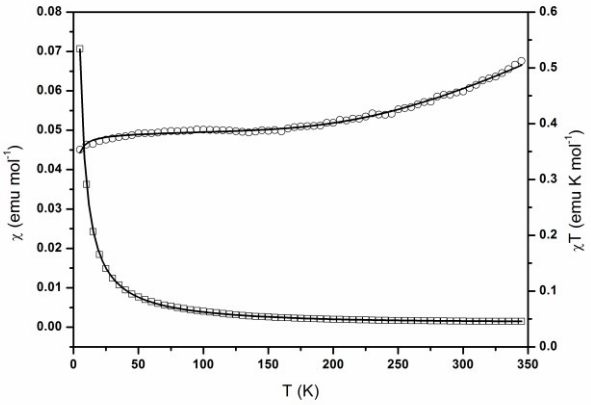

Figure 4 Temperature dependence of the magnetic susceptibility (square) and of the product of magnetic susceptibility with temperature (circle) for **2^{2+}** • 2 SbF_6^-. The black lines are the corresponding fitted curves.

In order to gain insight into the magnetic interaction between the manganese and the ligand radical we measured the magnetic susceptibility as a function of temperature on a solid sample of **2^{2+}** • 2 SbF_6^- (Fig. 4). At 345 K the value of the product of the magnetic susceptibility with temperature (χT) is 0.51 emu K mol^{-1} and decreases continuously upon cooling χT down to 160 K, where it reaches a plateau with a χT value of 0.38 emu K mol^{-1}. This behaviour indicates that an antiferromagnetic interaction operates between a high spin Mn(V) metal ion (S_{Mn} = 1) and the radical (S_{rad} = 1/2), with the χT value at the plateau corresponding well to the expected one for an S = 1/2 ground state spin. Then at very low temperature χT decreases again on cooling which is ascribed to the effect of antiferromagnetic intermolecular interaction. Accordingly, the data were simulated by considering the spin Hamiltonian:

$$\hat{H} = -2J\,\hat{S}_{Mn}\cdot\hat{S}_{rad}$$

From which the Van Vleck equation can then be derived using the Kambe approach:[19]

$$\chi = \frac{1.5}{T}\frac{e^{(-3J/kT)}+10}{4e^{(-3J/kT)}+8}$$

Then the intermolecular interactions (z'J') were incorporated in the molecular field approximation.[20] A good agreement between experimental and simulation was obtained considering an antiferromagnetic coupling J = -262(3) cm^{-1} and z'J'=-0.68(7) cm^{-1}, with g = 2.02.

Consistent with magnetic susceptibility measurements the X-Band EPR spectrum of a polycrystalline sample of **2^{2+}** • 2 SbF_6^- at both 6 K and 100 K is dominated by a sharp and isotropic resonance at g_{iso} ~ 1.99 (Fig. S14), which is assigned to the (S = ½) state. The quartet is located too high in energy, so that when this excited state is populated the relaxation time is too short. As a consequence the quartet could not be experimentally observed. The spectrum is similar in frozen CH_2Cl_2 solution, while the addition of TBAP allows for the resolution of the Mn hyperfine lines.[21] From simulation, the spin Hamiltonian parameters for the S = ½ system were determined at g_1 = 1.973, g_2 = 2.007, g_3 = 2.005, with the hyperfine coupling constants A_1 = A_2 = 0.54 mT and A_3 = 2.04 mT for a single Mn nucleus. The hyperfine coupling constants are much smaller than those reported for Mn(VI) complexes,[22] further supporting the radical character of **2^{2+}**.

In summary, we report the efficient synthesis of the electron rich NNN pincer ligand **1** and describe the crystal structure of **2^{2+}**, which is an extraordinarily stable non-oxo and non-nitrido manganese(V)-radical complex. Owing to the low oxidation potentials of our system and the versatility in the coordination mode we believe that **1** is a promising tool for investigating the detailed electronic structure of number of non-oxo metal complexes under unusually high oxidation states.

Aknowledgements

The authors thank the Labex Arcane (ANR-11-LABX-0003-01) for financial support, and Westgrid and 4D Labs for access to computational resources and XPS instrumentation, respectively.

Notes and references

1 (a) R. G. Hicks, *Angew. Chem. Int. Ed.,* 2008, **47**, 7393. (b) A. I. O. Suarez, V. Lyaskovskyy, J. N. H. Reek, J. A. van der Vlugt, B. de Bruin, *Angew. Chem. Int. Ed.,* 2013, **52**, 12510.

2 (a) I. G. Fomina, S. S. Talismanov, A. A. Sidorov, Y. A. Ustynyuk, S. E. Nefedov, I. L. Eremenko, I. I. Moiseev, *Russ. Chem. Bull., Int. Ed.,* 2001, **50**, 515. (b) A. K. Ghosh, S. M. Peng, R. L. Paul, M. D. Ward, S. Goswami, *J. Chem. Soc.,*

Dalton Trans., 2001, 336. (c) D. Herebian, E. Bothe, F. Neese, T. Weyhermüller, K. Wieghardt, *J. Am. Chem. Soc.,* 2003, **125**, 9116. (d) D. Herebian, K. Wieghardt, F. Neese, *J. Am. Chem. Soc.,* 2003, **125**, 10997. (e) E. Bill, E. Bothe, P. Chaudhuri, K. Chlopek, D. Herebian, S. Kokatam, K. Ray, T. Weyhermüller, F. Neese, K. Wieghardt, *Chem. Eur. J.,* 2005, **11**, 204. (f) K. Chłopek, E. Bill, T. Weyhermüller, K. Wieghardt, *Inorg. Chem.,* 2005, **44**, 7087. (g) K. Chłopek, E. Bothe, F. Neese, T. Weyhermüller, K. Wieghardt, *Inorg Chem.,* 2006, **45**, 6298. (h) M. van der Meer, Y. Rechkemmer, I. Peremykin, S. Hohloch, J. van Slageren, B. Sarkar, *Chem. Commun.,* 2014, **50**, 11104. (i) N. Leconte, J. Ciccione, G. Gellon, C. Philouze, F. Thomas, *Chem. Commun.,* 2014, **50**, 1918.

3 (a) A. Kochem, G. Gellon, N. Leconte, B. Baptiste, C. Philouze, O. Jarjayes, M. Orio, F. Thomas, *Chem. Eur. J.,* 2013, **19**, 16707. (b) A. Kochem, G. Gellon, O. Jarjayes, C. Philouze, N. Leconte, M. van Gastel, E. Bill, F. Thomas, *Inorg Chem.,* 2014, **50**, 4924.

4 (a) Y. Nakato, M. Oazki, H. Egawa, H. Tsubomura, *Chem. Phys. Lett.,* 1971, **9**, 615. (b) R. Gross, W. Kaim, *Inorg. Chem.,* 1987, **26**, 3596.

5 C. Wurster, *Ber. Dtsch. Chem. Ges.,* 1879, **12**, 522.

6 (a) A. Y. Girgis, A. L. Balch, *Inorg. Chem.,* 1975, **14**, 2724. (b) C. G. Pierpont, C. W. Lange, *Prog. Inorg. Chem.,* 1994, **41**, 331. (c) P. Chaudhuri, M. Hess, T. Weyhermüller, K. Wieghardt, *Angew. Chem. Int. Ed.,* 1999, **38**, 1095. (d) C. L. Simpson, S. R. Boone, C. G. Pierpont, *Inorg. Chem.,* 1989, **28**, 4379. (e) G. Szigethy, D. W. Shaffer, A. F. Heyduk, *Inorg. Chem.,* 2012, **51**, 12606. (f) G. Szigethy, A. F. Heyduk, *Dalton Trans.,* 2012, **41**, 8144.

7 (a) J. Breitenfeld, J. Ruiz, M. D. Wodrich, X. Hu, *J. Am. Chem. Soc.,* 2013, **135**, 12004. (b) J. Breitenfeld, M. D. Wodrich, X. Hu, *Organomet.,* 2014, **33**, 5708.

8 (a) A. I. Nguyen, K. J. Blackmore, S. M. Carter, R. A. Zarkesh, A. F. Heyduk, *J. Am. Chem. Soc.,* 2009, **131**, 3307. (b) A. I. Nguyen, R. A. Zarkesh, D. C. Lacy, M. K. Thorson, A. F. Heyduk, *Chem Sci.,* 2011, **2**, 166. (c) R. F. Munha, R. A. Zarkesh, A. F. Heyduk, *Inorg. Chem.,* 2013, **52**, 11244.

9 The large ΔEp measured for the first oxidation wave is indicative of a proton-coupled to electron transfer.

10 TD-DFT calculations predict for **2** two low energy electronic excitations at 1739.83 nm (f_{osc} = 0.0243) and 1084.53 (f_{osc} = 0.0481). For $\mathbf{2}^{2+}$ an electronic excitation is predicted at 1142.31 nm (f_{osc} = 0.0672), which accounts for the NIR tail experimentally observed. The associated Natural Transition Orbitals (NTOs) are shown in Tables S1 and S2.

11 (a) S. K. Larsen, C. G. Pierpont, *J. Am. Chem. Soc.,* 1988, **110**, 1827. (b) A. S. Attia, C. G. Pierpont, *Inorg. Chem.,* 1998, **37**, 3051. (c) H. Chun, P. Chaudhuri, T. Weyhermüller, K. Wieghardt, *Inorg. Chem.,* 2002, **41**, 790.

12 J. Ciccione, N. Leconte, C. Philouze, D. Luneau, F. Thomas, *Inorg. Chem.,* 2016, **55**, 649.

13 E. Paparazzo, *Catal. Today*, 2012, **185**, 319.

14 T. A. Furtsch, L. T. Taylor, *Inorg. Chim. Acta,* 1982, **61**, 211.

15 R. E. Schreiber, H. Cohen, G. Leitus, S. G. Wolf, A. Zhou, L. Que, Jr., R. Neumann, *J. Am. Chem. Soc.,* 2015, **137**, 8738.

16 W. P. Kilroy, S. Dallek, J. Zaykoski, *J. Power Sources,* 2002, **105**, 75.

17 M. Ding, G. E. Cutsail Iii, D. Aravena, M. Amoza, M. Rouzieres, P. Dechambenoit, Y. Losovyj, M. Pink, E. Ruiz, R. Clerac and J. M. Smith, *Chem. Sci.*, 2016, **7**, 6132.

18 The use of a Mn(IV) state as an initial guess converges to the Mn(V)-radical $^{4}\mathbf{[2]}^{2+}$ solution.

19 K. Kambe *J. Phys. Soc. Jpn* 1950, **5**, 48.

20 A. P. Ginsberg, M. E. Lines in "Magnetic Exchange in Transition Metal Complexes. VIII. Molecular Field Theory of Intercluster Interactions in Transition Metal Cluster Complexes".

21 For the electrochemically generated $\mathbf{2}^{2+}$ (in CH_2Cl_2 + 0.1 M TBAP) a new broad feature is observed at g ~ 2, associated to a shoulder at g ~ 4 (150 mT) in the temperature range 6-20 K. These features are indicative of a high spin state. This signal is not detected when a chemically generated sample is dissolved in neat CH_2Cl_2, while it is barely visible for microwave powers larger than 20 mW and 6 K when a chemically generated sample of $\mathbf{2}^{2+}$ 2 SbF_6^- is dissolved in CH_2Cl_2 + 0.1 M TBAP (see ESI). Hence, the interactions between the counter-ions and the complex (presumably through the NH groups) likely alter the quartet-doublet energy gap and/or the electronic structure of $\mathbf{2}^{2+}$.

22 (a) J. Bendix, K. Meyer, T. Weyhermüller, E. Bill, N. Metzler-Nolte, K. Wieghardt, *Inorg. Chem.* 1998**, 37**, 1767. (b) K. Meyer, J. Bendix, N. Metzler-Nolte, T. Weyhermüller, K. Wieghardt, *J. Am. Chem. Soc.* 1998**, 120**, 7260. R. M. Clarke, T. Storr, *J. Am. Chem. Soc.* 2016, **138**, 15299.